Geophys. J. Int. (2007) **169,** 659–666 doi: 10.1111/j.1365-246X.2007.03356.x

Imaging the basin and fault geometry from the multichannel seismic reflection data in the Tekirdağ Basin, Marmara Sea, Turkey

Zakir Kanbur,[1] Ömer Alptekin,[2] Murat Utkucu[3] and Süveyla Kanbur[4]

[1] *Suleyman Demirel University, Department of Geophysics, Isparta, Turkey. E-mail: zakir@mmf.sdu.edu.tr*
[2] *Istanbul University, Department of Geophysics, Avcılar, Istanbul*
[3] *Yuzuncu Yıl University, Department of Geology, 65080, Kampus, Van, Turkey*
[4] *Suleyman Demirel University, Department of Geology, Isparta, Turkey*

Accepted 2007 January 12. Received 2007 January 10; in original form 2006 March 7

SUMMARY

Determination of the fault geometry in the Marmara Sea has been a major problem for the researchers after the occurrence of the 1999 August 17 Golcuk ($M = 7.4$) earthquake. To shed a light to the problem we applied the pre-stack Kirchhoff depth migration technique to the multichannel seismic reflection data of three profiles to investigate the basin and fault geometry in the Tekirdağ Basin in the western Marmara Sea. The boundary of the basin and its sediments were revealed in N–S and NE–SW directions in depth sections. We identify major fault types involving these structures at different locations in Tekirdag Basin showing that the basin is developed under their movement. The North Anatolian Fault is imaged and interpreted as transtensional character at the centre of the Tekirdağ Basin that is symmetrically divided with a large distributed zone. The fault plane is imaged through the depth of 2 km dipping to the north with 90° in the upper 350 m and 82° in the lower part. The basin thickness reaches about 2.5 km at that point. Syn-transform sediments of the basin are disturbed by some normal faults dipping to the north. These faults are represented by notable displacements of the reflections which prompted us to consider them as a potential tsunami source if they move during a large earthquake along the major fault. Another major fault is identified at the westernmost of the basin. Because it shows the same character as Ganos fault, it might be submarine part of it. It has reverse component with the dip angle of 65° to the north and trending along the western flank of the basin. A reverse fault is identified appearing in low angle (∼20°) surrounding the edge of the submarine slide at southwest of the basin. From its geometry it is interpreted as a local fault formed between two main faults. From the sketch of the basin and the fault geometry obtained from the images we suggest that the basin should be formed by a pull-apart system.

Key words: imaging technique, Marmara Sea, North Anatolian Fault system, pre-stack Kirchhoff depth migration, seismic imaging, Tekirdağ Basin.

1 INTRODUCTION

The main reason of the complex deformations in the crust of the Marmara Sea region is the right lateral motions along the North Anatolian Fault System (NAFS) which was formed due to the relative motion among the African, Arabian and the Eurasian plates. As a result of relative motions of African and Arabian plates with respect to the Eurasian plate, the Arabian plate collides with the Eurasian plate, forcing the Anatolian microplate to move westward, and the African plate subducts beneath the Anatolian plate (Fig. 1). These movements had formed the approximately 1500 km long, seismically very active, dextral NAFS which is the major tectonic component of Turkey and the surrounding area. It joins the sinistral East Anatolian Fault System (EAFS) and creates a triple junction at Karlıova in eastern Turkey (Ketin 1968; McKenzie 1972; Şengör 1979). The westward motion of the Anatolian plate along the NAFS is about 24 mm y^{-1} according to GPS studies (McClusky *et al.* 2000).

The NAF splits into three branches in the Marmara region (Barka & Kadınsky-Cade 1988) (Fig. 2). However, more recent studies such as Armijo *et al.* (2002), Meade *et al.* (2002) and Flerit *et al.* (2003) indicate two strands. The Northern branch is lying between Izmit Gulf in the east and the Aegean Sea in the west. Its submarine section, referred as Marmara fault in the present study, is active and has potential seismic hazard for surrounding areas. It stands in Marmara region that has most crowded population and the most economic importance in Turkey. Particularly, following the 1999 August 17 Izmit earthquake, Marmara fault has been subject to many

© 2007 The Authors
Journal compilation © 2007 RAS

Downloaded from https://academic.oup.com/gji/article-abstract/169/2/659/625546 by Suleyman Demirel Uni user on 17 April 2020

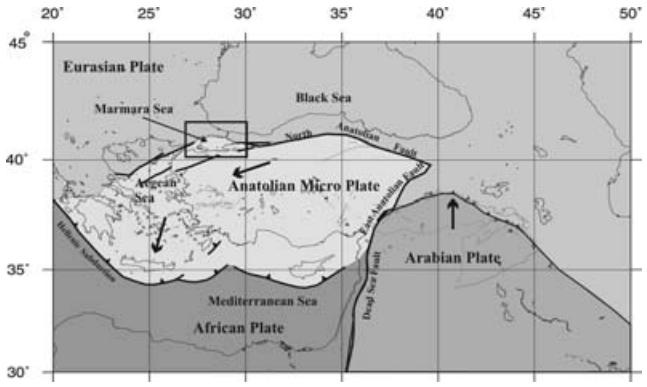


Figure 1. Active tectonics map of eastern Mediterranean region and geological setting of the Marmara Sea. The solid arrows indicate the direction of motion of the lithospheric plates with relative to Eurasian plate. The large rectangle indicates the map area of Fig. 2.

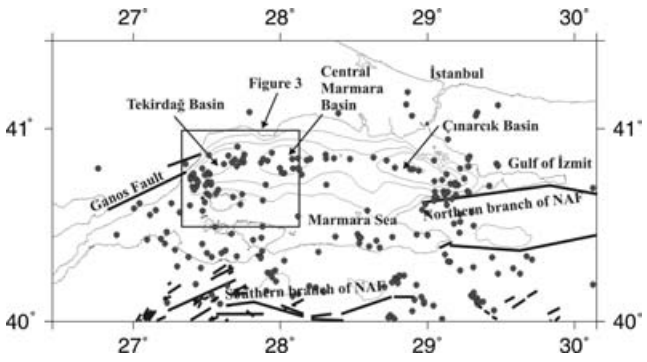


Figure 2. Active fault map of the Marmara Sea and surrounding areas showing seismotectonic setting of Tekirdağ Basin. Fault locations are modified from General Directorate of Mineral Research and Exploration (MTA). Earthquake locations (Ms > 2.3) in the Marmara Sea obtained from Kandilli Observatory and Earthquake Research Institute, covering a period that extends from 2002 to 2004.

studies and several models have been suggested for its geometry and structure. It however remains controversial (Barka & Kadınsky-Cade 1988; Wong *et al.* 1995; Okay *et al.* 1999, 2000; İmren *et al.* 2000; Le Pichon *et al.* 2001).

Wong *et al.* (1995) and Parke *et al.* (1999) suggested that mainly the N–S extension tectonics in the Aegean Sea and western Anatolia and NAFS is responsible for the tectonics of the Marmara Sea. However, Flerit *et al.* (2003) showed through GPS velocity field modelling that there is no extension perpendicular to the strike of the NAFS and deformation in the Marmara Sea resulting purely from the pull-apart geometry of it. GPS velocity field measurement and field studies showed that the NAF makes a 17° bend through south in the western Marmara Region (Okay *et al.* 2004).

The properties of NAFS beneath the Marmara Sea and its geometry are revealed by seismic, seismologic and bathymetric data. The researchers of several studies claimed that NAFS in this area extends as a thoroughgoing fracture zone (Pınar 1942; Şengör 1979; Şengör *et al.* 1985; Le Pichon *et al.* 1999). The Marmara Sea is cut by E–W grabens (Ketin 1968; McKenzie 1972; Crampin & Evans 1986; Smith *et al.* 1995), or the NAF in this area extends as a combination of en-echelon strike-slip fault segments with resulting pull-apart basins (Barka & Kadınsky-Cade 1988; Wong *et al.* 1995; Şengör *et al.* 1999; Armijo *et al.* 2000, 2002). Previous studies have focused especially on the basin development. However, the 1999 August 17 İzmit earthquake motivated the researchers to investigate the nature of the active faults of the northern Marmara Sea tectonics. Thus, some new studies regarding the determination of active faults have been done by interpreting the recently collected seismic reflection data in the Marmara Sea. Okay *et al.* (1999) suggested that the Marmara fault system consists of three faults segments, which are 15, 105 and 45 km in length, respectively, trending from west to east. İmren *et al.* (2000) claimed the fault system to be called Marmara fault consisting of two main segments as 80 km in the west and 65 km in the east. Le Pichon *et al.* (2001) suggested that the active dextral NAFS beneath the Marmara Sea connects to the dextral fault segments that produced the earthquakes of the 1999 August 17 İzmit in the east and the 1912 August 9 Murefte-Şarköy in the west. However, Armijo *et al.* (2002), in contrary of one single dextral fault model, considers a smaller submarine pull-apart geometry linking the fault ruptures of the 1912 and 1999 earthquakes within the larger Marmara pull-apart. This model requires transtensional tectonic regime as proposed previously by Barka & Kadınsky-Cade (1988) and Wong *et al.* (1995). The transtensional regime caused three deep basins (Çınarcık, Central and Tekirdağ Basins from east to west) with depths over 1000 m under the Northern Marmara Sea (Fig. 2). Armijo *et al.* (2005) observed submarine scarps beneath the Marmara Sea by an extensive study and suggested that the 1912 Ganos rupture is crossed the Ganos restraining bend into the Marmara Sea for 60 km with a right lateral slip of 5 m and ending in Central basin as step-over. Thus they suggested that the total length of the 1912 Ganos rapture is 140 km instead of 50 km as previously thought.

As it is seen from the literature, the researchers proposed various fault models through interpreting various seismic reflection data sets collected in the region to explain the nature of the fault system beneath the Marmara Sea. However, there has not been a compromise about the properties of the fault system involving the structure of Marmara Sea tectonics. This fact indicates that the diversity of the proposed models may be partly due to the limitation of the conventional stacking technique used to explain the complex structures in the Marmara Sea tectonics.

In 1997 September, the General Directorate of Mineral Research and Exploration (MTA) of Turkey collected multichannel seismic reflection data by the survey ship Seismic 1 along several profiles in Tekirdağ Basin of the Marmara Sea. The collected data were interpreted applying only the conventional seismic processing technique including seismic stacking and time migration (Okay *et al.* 1999). In the standard seismic processing technique it is assumed that strong lateral velocity variation does not exist. On the other hand, complex structures such as the Marmara Sea having both vertical and horizontal faults lying beneath the Marmara Sea violate these assumptions in seismic stacking technique (Yılmaz 1987). In such areas, the data are not fully interpretable by applying the standard reflection processing techniques and thus some other techniques must be used performing under fewer assumptions.

Pre-stack Kirchhoff depth migration is the technique that inverts the multichannel reflection data to the migrated depth section. Several studies showed that pre-stack Kirchhoff depth migration technique is capable for imaging the complex structure better than the conventional seismic reflection processing techniques (Louie *et al.* 1988; Louie & Qin 1991; Honjas 1995; Kanbur *et al.* 2000). To determine the geometry and neo-tectonics properties of the NAFS extending in the Tekirdağ Basin, we applied the pre-stack Kirchhoff depth migration technique to the multichannel seismic reflection data collected along three profiles in Tekirdağ Basin, the Marmara

Downloaded from https://academic.oup.com/gji/article-abstract/169/2/659/625546 by Suleyman Demirel Uni user on 17 April 2020

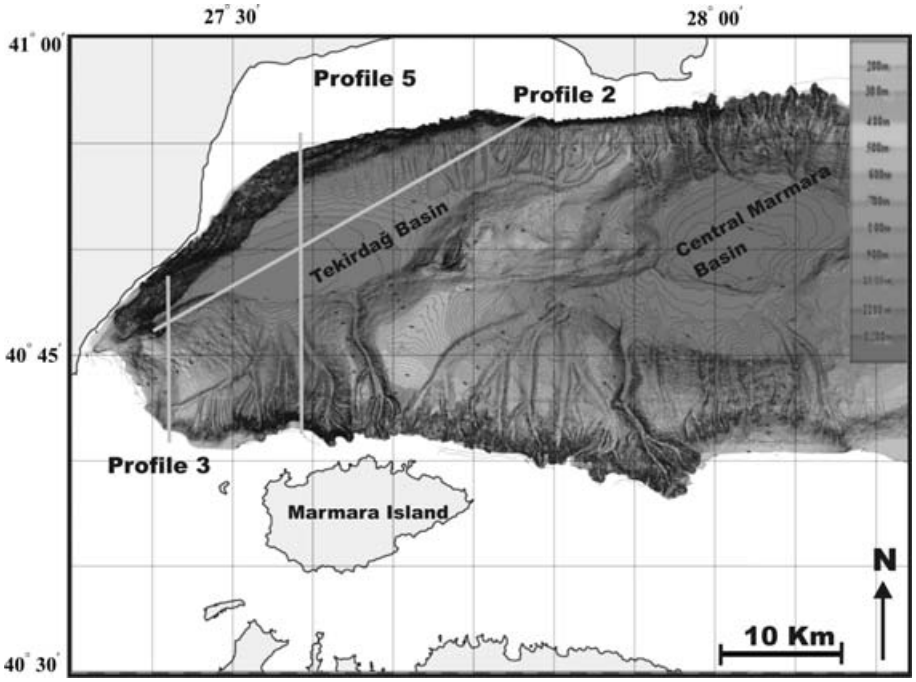


Figure 3. Bathymetric map of Tekirdağ Basin and surrounding areas. Straight lines show multichannel reflection data profile to which pre-stack migration technique is applied. The map was modified from internet site (http://www.ifremer.fr/drogm_uk/marmara/accueil_2.htm).

Sea, in addition to the standard seismic interpretation techniques including seismic stacking and time migration (Fig. 3). This study is aimed to reinterpret the reflection data to give additional information regarding the fault geometry in the area.

2 METHOD

2.1 Field procedure

Among the MTA profiles in Tekirdag basin, we selected three profiles numbered 2, 3 and 5 in Fig. 3. One of them cut the basin in SW–NE direction and two of them cut the basin in N–S direction (Fig. 3). These profiles may represent the properties of the basin and the faults involving the structure.

A 96 channel streamer seismic reflection survey collected data at 12.5 m station and 50-m source interval along the profiles 2, 3 and 5 using air gun source array of 1380 cubic inches. The field acquisition parameters are given in Table 1.

Table 1. Field acquisition parameters.

Acquisition parameters	
Date	1997 September
Profiles	2 (SW–NE), 3 and 5 (N–S)
Spread type	Off-and
Number of channels	96
Hydrophone spacing	12.5 m
Source spacing	50 m
Source type	Air gun 1380 cubic inches
Minimum offset	150 m
Maximum offset	1337.5 m
Nominal fold	12
Sampling rate	2 ms
Record length	8 s

2.2 Data processing

We first applied the common midpoint (CMP) stacking and time migration techniques to obtain velocity information regarding the reflectors underlying the Tekirdağ Basin in Marmara Sea. The processing flow was very similar to that used for ordinary seismic data interpretation techniques that include pre-processing, stacking and time migration. Three main sources of noise are visible in the data. One is the first arrival from the seawater, the second is multiple reflections and the last one is sidewall reflections. Sideswipe off the nearby steep slope of the sea shelf makes the raw data more complex.

We applied bandpass frequency filtering with 20 percent taper in the range of 10–95 Hz. This process also makes the multiple reflections weaker but we do not spend extra care for removing them from the data because the signal level is not significant. Muting is also applied to all data records to remove direct and refracted arrivals to enhance the earlier reflections. Finally, the basic processing sequence, trace equalization gain, bandpass filtering, muting, applying geometry, NMO velocity analysis, CMP-stack and migration, is implemented.

To obtain the CMP stacking sections of the profiles 2, 3 and 5 collected in Tekirdağ Basin, the best stacking velocity model has to be identified by performing NMO velocity analysis. Velocities picked from constant velocity test stacks made at 100 $m\,s^{-1}$ increment ranged from 1500 to 2500 $m\,s^{-1}$. After choosing the best stacking velocities as a function of time at several different shot locations, we finally obtained the CMP-stacked sections. We applied a time migration with 1700 $m\,s^{-1}$ average velocity to the stacking sections and obtained migration sections collecting all diffractions appeared on the stacking sections to a point reflector (not shown here).

2.3 Pre-stacked migration

A number of studies demonstrated that pre-stacked migration may efficiently be used to determine the geometry of complex structures

© 2007 The Authors, *GJI*, **169,** 659–666
Journal compilation © 2007 RAS

Downloaded from https://academic.oup.com/gji/article-abstract/169/2/659/625546 by Suleyman Demirel Uni user on 17 April 2020

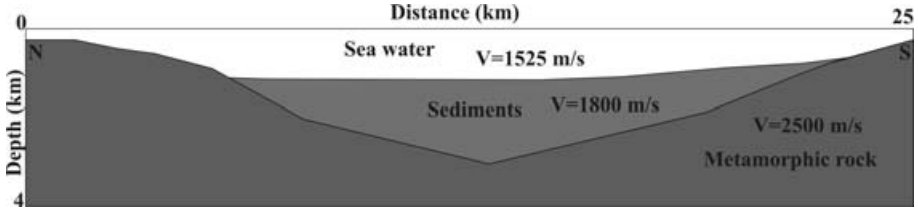


Figure 4. An example of the 2-D velocity model of profile 5. It is obtained from the stacking velocities converted to interval velocities using Dix equation (Dix 1965). Traveltimes matrix calculated using the velocity model by Vidale's (1988) finite difference solution of the eikonal equation in two dimensions. The internal velocities are not calculated in sediments of the basin due to lock of adequate velocity gradient.

that involve faulting, folding, etc. (Louie *et al.* 1988; Louie & Qin 1991; Honjas 1995; Kanbur *et al.* 2000). An appropriate result from stacking technique is only possible using a number of assumptions regarding the properties of subsurface reflectors in the earth conflict. When these assumptions are violated, the seismic sections may not be fully interpretable. In conventional processing, NMO and CMP stack techniques ideally require laterally homogeneous and horizontally layered media. In case of high degree lateral heterogeneity and dipping layers, the two processes perform poorly (Jain & Wren 1980). Tekirdağ Basin is characterized by strong lateral heterogeneity and steeply dipping layers. Thus, the pre-stack Kirchhoff depth migration is a process that can efficiently handle the geometric irregularity and lateral heterogeneities.

The pre-stack migration algorithm used in this paper is the Kirchhoff summation method (Louie *et al.* 1988; Louie & Qin 1991; Honjas 1995; Kanbur *et al.* 2000). The method requires traveltime curves to be computed from a velocity model. We used interval velocities obtained from stacking velocity picks as a velocity model to calculate traveltimes using Vidale's (1988) finite difference solutions of the eikonal equation. All stacking picks corresponding to the shot records were obtained and calculated for interval velocities. Then, a separated velocity model of each shot record were prepared and calculated for the traveltime curves for each record. Fig. 4 shows the velocity model of the profile. This process was applied to all reflection data of three profiles.

Fig. 5 summarizes the Kirchhoff pre-stack imaging procedure. The unsorted data traces are mapped by Kirchhoff pre-stack imaging into a depth section by computing the traveltime from the source to the depth point and back to the receiver, through the velocity model. The velocity model has 100 m s^{-1} velocity, which corresponds to a depth error of 5 percent in the depth section. The traveltime calculation includes turning rays, which allows for the imaging reflections of dipping structures. Within the traveltimes down to and up from every point in the data, the value of the seismogram is summed into the section at the depth point. Coherent and continuous events at that time will constructively interfere, which will indicate the presence of earth structure in the depth section. The tomographic sum, or the summation of arrival times, may be made in any order, since the Kirchhoff summation methods embraces the geometrical configuration of the source, receiver and the reflector as a function of time. Pre-stack Kirchhoff depth migration was applied to 750 records of profile 2, 300 records of profile 3 and 500 records of profile 5. Coherent and continuous events indicate structure in the depth section. Figs 6–8 show the results of the pre-stack Kirchhoff depth migration sections. The sections have best presentations in three times of vertical exaggeration.

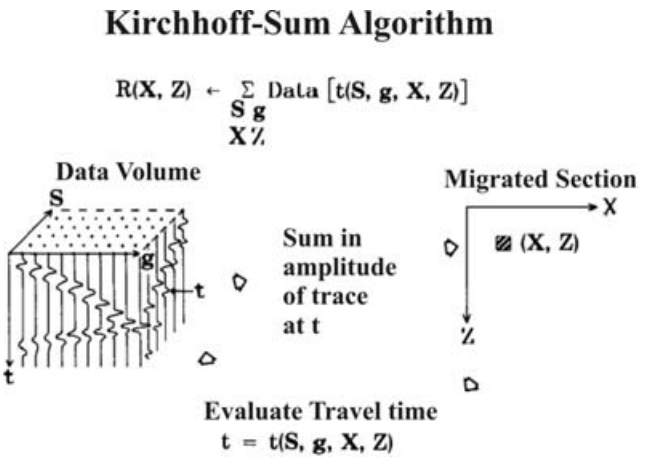


Figure 5. Summary of the processing of pre-satck Kirchhoff depth migration technique. The velocity model shown in Fig. 4. was obtained from stacking velocities that are converted to interval velocities using Dix equation (Dix 1965). Once obtained best model the traveltimes are calculated down to and up from each depth point, the value of the seismogram at that time than summed into the section at the depth point: This is done as a traveltime calculation for each recorded receiver pair (S, g) over each point (X, Z) in some depth section. The amplitude of the recorded trace at that time is then summed into the point of the depth section. The figure modified from Louie *et al.* (1988).

3 RESULTS AND DISCUSSION

Tekirdağ Basin is westernmost strike-slip depressions in the Marmara Sea (Fig. 2). Its shape is rhomboidal with 40 km in length and 15 km in width, having the long axis subparallel to the NAFS that divides the basin into two parts at the centre. The basin is bounded by the boundary faults in the N–S directions, by Ganos Mountain and by the central high distinguishes Tekirdağ and Central Basins in the east, and mostly interpreted as an extensional basin (Ergün & Özel 1995; Wong *et al.* 1995; Okay *et al.* 1999; Parke *et al.* 1999; İmren *et al.* 2000; Le Pichon *et al.* 2001; Armijo *et al.* 2002) (Figs 2 and 3).

The images of pre-stack Kirchhoff (Figs 6 and 7) show that the basin is inclined to the south about ∼0.4° and to the southwest about ∼0.3°. It is flanked from both sides by ∼13°–22° escarpments and makes an unconformity with syn-tectonic sediments, which increasingly declined by depth towards south and are cut by NAFS at the depth centre of the basin. The escarpment of sediments and metamorphic rock intersect each other in the depth of about 3900 m (Fig. 6). Based on this depth level, the maximum depth of sediment accumulation is approximately 2566 m. The basin seems asymmetric and is distinguished by Pliocene-Quaternary syn-transform strata from metamorphic rocks in the south and by Eocene-Oligocene clastic sequence in the north (Wong *et al.* 1995; Okay *et al.* 1999). The regional stratigraphic section obtained from the data on land consists of two Tertiary series (Kopp *et al.* 1969; Turgut *et al.* 1991; Sümengen & Terlemez 1993; Görür & Okay 1996). The lower one

Downloaded from https://academic.oup.com/gji/article-abstract/169/2/659/625546 by Suleyman Demirel Uni user on 17 April 2020

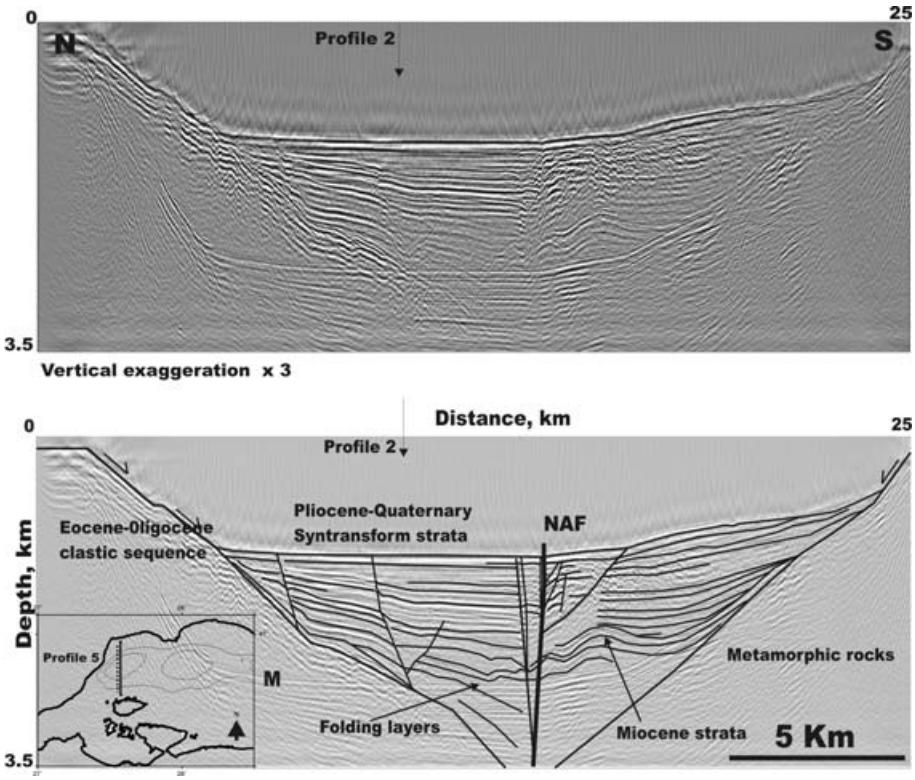


Figure 6. Uninterpreted and interpreted pre-stack Kirchhoff depth migrated seismic reflection section of profile 5. M indicates multiple reflections. NAF: North Anatolian Fault. The artefact patterns produced from the Kirchhoff algorithm are evident on the muted side. The technique produced good images where strong lateral gradients exist. Strong deformation is visible around NAF that is well imaged as a vertical interface through 350 m depth from the sea bottom.

is a siliciclastic sequence of middle Eocene age and the upper one is Oligocene age.

Okay *et al.* (1999) and Seeber *et al.* (2004) defined the NAF as dipping north about ∼70° and ∼67° and getting stepper at depth (fig. 9 in Okay *et al*., 1999; fig. 3b in Seeber *et al*. 2004). On the contrary, the pre-satck Kirchhoff depth migration image of the profile 5 shows different picture (Fig. 6). The image defines the NAF as appearing almost 90° from the sea bottom to the depth of 350 m and its angle changes to about 82° north dipping at the deeper part. A small displacement due to the fault is visible at the sea bottom. Beginning from that point, a large distribution zone gradually takes place by increasing depth and therefore NAFS at Tekirdag Basin can be defined by an interface at upper part and by the truncation of sediments at lower part. The upper disturbed zone is diverged by the fault and it stands upwardly concave. This fact may be evaluated as an evidence of the NE–SW extension of Marmara region as indicated by the modelling of GPS velocity field (Armijo *et al.* 2002; Flerit *et al.* 2003). Some minor faults closely accompany to the main fault, however these all look inactive for long time due to lock of any trace at the surface of the sea bottom. This indicates a slow process of the basin extension as indicated also by Flerit *et al.* (2003) and Okay *et al.* (2004).

Syn-transform sediments consist of various units through the depth. The shallower part of these units is laying relatively horizontal and onlap to the both edges of the basin. Northern part of the basin is sin-rift at greater depths and reflections are almost parallel. The northern part is relatively undisturbed but the southern part is very similar to a transpressional push up structure as indicated by Wong *et al.* (1995). According to Seeber *et al.* (2004) and Okay *et al.* (2004) the NAFS is responsible for growth of the Tekirdağ Basin due to progressive tilting of syn-tectonic sediments. Fig. 6 also shows that syn-transform strata of Tekirdağ Basin are disturbed asymmetrically. Syn-transform sediments of south part also show two different characters as lower and upper parts. The reflections appeared on upper part are relatively undisturbed. The lower part (>600 m depth) contains well-stratified section that was interpreted as unconformity (Ergün & Özel 1995; Yazman 1997). The edges of the reflections in this section appear as folding and are truncated towards the fault zone indicating strike-slip fault.

The northern part of syn-transform sediments is disturbed by a few normal faults dipping towards north. As seen in Fig. 6 the faults are represented by some significant displacements of reflections. These faults are the component of the extensional tectonic regime of Tekirdag Basin. If the NAFS fault creates a large earthquake at Tekirdag basin, it may be assumed these normal faults to move down as land slices and thus this vertical movement may create a tsunami threatening the coasts of Marmara Sea. The probability of a tsunami is not farfetched considering historical records of tsunamis in the Marmara Sea (Ambraseys 2002). The magnitude of the tsunami will be depending on the slip rate on the normal fault.

At the west of the basin, the reflections from syn-transform strata are not ended by the surface of the steep wall of submarine valley but continue towards its interior and meet the interface of the sediments and the Eocene-Oligocene clastic sequence at data records and stacking section (Fig. 7). Due to the profile location, the reflections arrivals from the sediments are represented in the data as sidewall reflections. These are mostly disappeared in the section of the profile 2 shown in B using more appropriate velocity model considering geological sequence. Okay *et al.* (1999) showed Ganos fault (in their fig. 10-11E) as a low angle reverse fault as considering the

© 2007 The Authors, *GJI*, **169,** 659–666
Journal compilation © 2007 RAS

Downloaded from https://academic.oup.com/gji/article-abstract/169/2/659/625546 by Suleyman Demirel Uni user on 17 April 2020

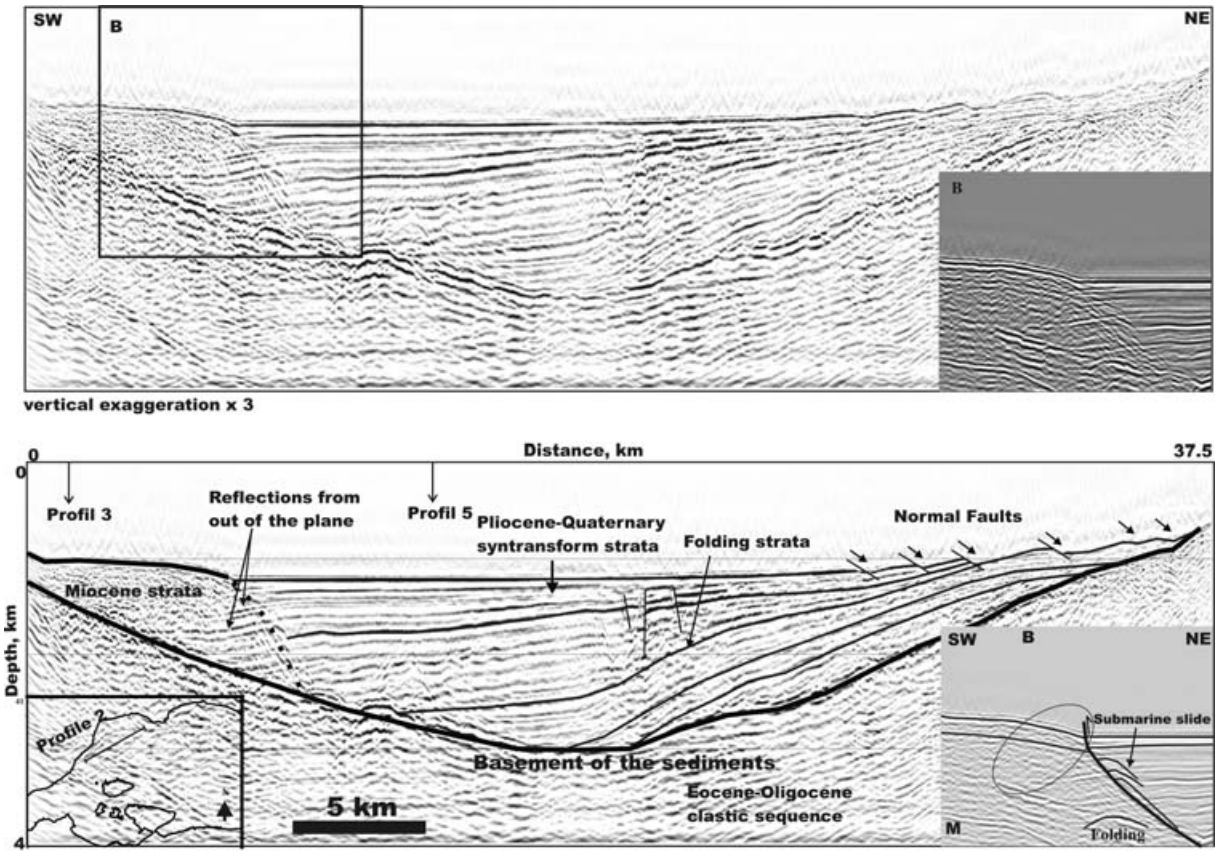


Figure 7. Uninterpreted and interpreted pre-stack Kirchhoff depth migrated seismic reflection section of profile 2. M indicates multiple reflections. The layers and the basement of the sediments are well imaged. The out of the plane reflections appearing on the upper left of the section mostly disappeared on the section shown in B. Using different velocities obtained by a careful velocity analysis.

side reflections. However, our image of profile 2 does not suggest any indication for Ganos fault to exist at that location. The sharp displacements at the sediments and submarine valley and on the interface at the depth indicate a reverse fault with a low angle about 20° that should be little higher than appeared due to data profile crossing the fault direction with a low angle (Fig. 3).

Fig. 8 shows the image of profile 3. The data records in profile are contaminated by strong reflections coming from the dipping bottom of the sea. As shown in Fig. 3, the profile 3 is perpendicular to the slope of Ganos Mountain (Eocene Oligocene clastic sequence) and the submarine slope. These topography results side reflections that appear as an interface continuing under the sea bottom. Okay *et al.* (1999) defined the side reflections as low angle interface appearing between Eocene Oligocene clastic sequence and Miocene strata in their seismic section (figs 11a and d) and misinterpreted this event as Ganos fault. Kirchhoff depth imaging technique disordered the coherence of the side reflections that are mostly disappeared on the section. This allowed locating the fault to its true location as appeared at the north part of the profile 3 (Fig. 8). It has a reverse component steeply north dipping with 65°. Reverse component can be seen on the land part of this fault, which dips quite steeply to the north (Okay *et al.* 2004). We interpret that this fault should be the extended part of the Ganos fault. Fig. 9 summarizes the main differences identified between present and previous studies.

All the faults identified from the images are presented in the map view of Fig. 10. Our images suggest two main strands of the NAF existing at the Tekirdağ Basin. First one is highly vertical with normal component and is trending ENE–WSW at the centre of the basin and the second one is also highly vertical but with reverse component trending WNW–WSE. We define these faults steeper than previous researchers (Okay *et al.* 1999; Demirbağ *et al.* 2003; Seeber *et al.* 2004). This is due to using different techniques employing under different assumptions as it is explained in method section. Between two faults a reverse fault zone appears in low angle (∼ 20°). It consists of en-echelon fault system at the edge of the Miocene submarine slide towards east (Le Pichon *et al.* 2001; Demirbağ *et al.* 2003). The geometrical and structural properties of these faults show that they are formed between the NAF and the Ganos fault as secondary faults.

4 CONCLUSION

The multichannel seismic reflection data collected along three profiles in Tekirdağ Basin, Marmara Sea were interpreted by applying pre-stack Kirchhoff depth migration techniques. The technique images the basin and fault geometry from the profiles with some differences from the previous studies. The boundary of the basin and its sediments are revealed in N–S and NE–SW directions in depth sections. We identified major fault types involving this structure at different locations in Tekirdag Basin. The NAFS is imaged at the centre of the Tekirdağ Basin showing that it divides the basin symmetrically with a large distributed zone. The fault plane is imaged through the depth of 2 km dipping to the north with the angle of

Downloaded from https://academic.oup.com/gji/article-abstract/169/2/659/625546 by Suleyman Demirel Uni user on 17 April 2020

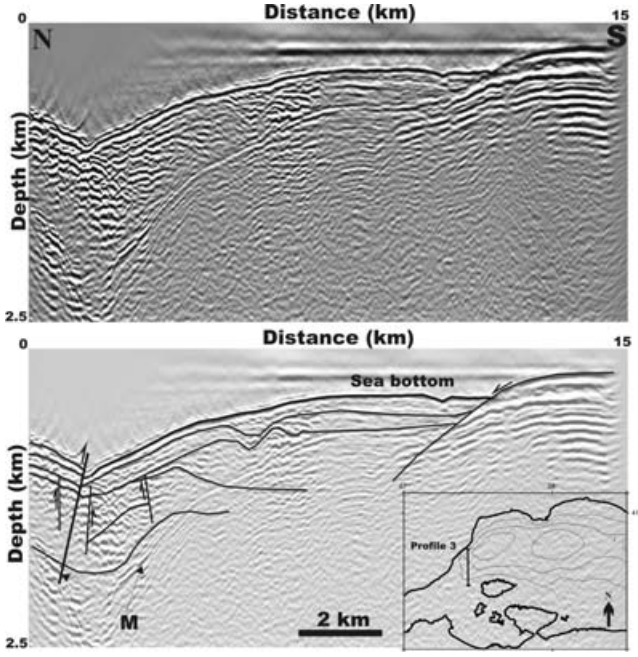


Figure 8. Uninterpreted and interpreted pre-stack Kirchhoff depth migrated seismic reflection section of profile 3. M indicates multiple reflections. The artefact patterns produced from the Kirchhoff algorithm are evident on the muted side. Ganos fault appears with angle of 65° at the area where vertical strong deformation exists.

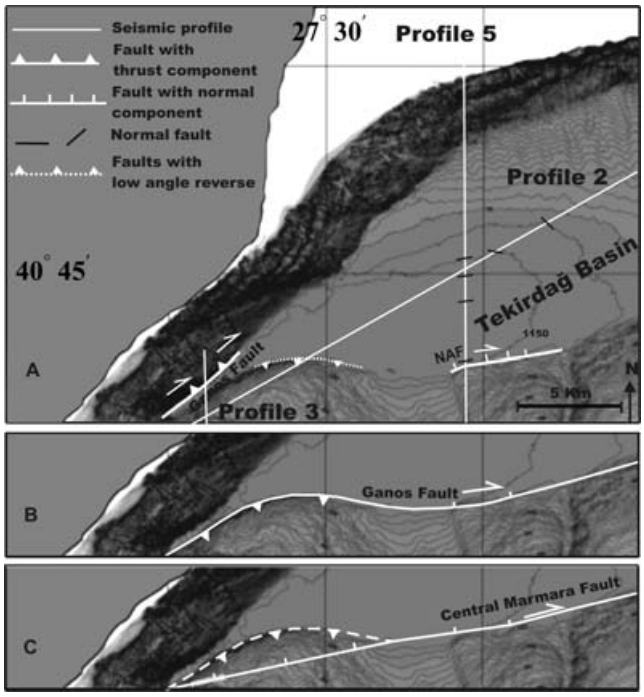


Figure 10. (a) Map shows profile location and corresponding fault location interpreted from the seismic images of the seismic reflection data profiles in the study. Short black lines indicate the normal faults encountered on the sediments of Tekirdağ Basin. The map was modified from internet site (http://www.ifremer.fr/drogm_uk/marmara/accueil_2.htm). (b) After Okay *et al.* (1999). (c) After Okay *et al.* (2004).

90° in upper 350 m and 82° in lower part. On the contrary, previous studies defined Ganos fault with angle of ∼70° and its lower part is stepper. The basin thickness reaches about 2.5 km at that point. Syn-transform sediments of the basin are disturbed by some normal faults dipping to north. These faults with determined displacement in the images have significant potential for producing tsunami during an event along NAFS. Upwardly concave disturbed zone and the dipping normal faults to north indicate southward extension. Another major fault is identified at the westernmost of the basin. This fault with reverse component shows the same character with Ganos fault. The fault appears on the image with the angle of 65°. Our interpretation is totally different from the previous study at this area that Ganos fault is defined by an interface between Eocene Oligocene clastic sequence and Miocene strata. We show that this event, in fact, resulted from the steep submarine wall of the basin. Also previous study in this area showing Ganos fault on the section of profile 2, however we do not find any event regarding Ganos fault. Instead of that, a reverse fault is identified between two main faults appearing in low angle (∼20°) at the edge of the Miocene submarine slide. It is interpreted as a local fault formed between two main faults. From the sketch of the basin and the fault geometry obtained from the images we suggest that the basin is formed by a pull-apart system.

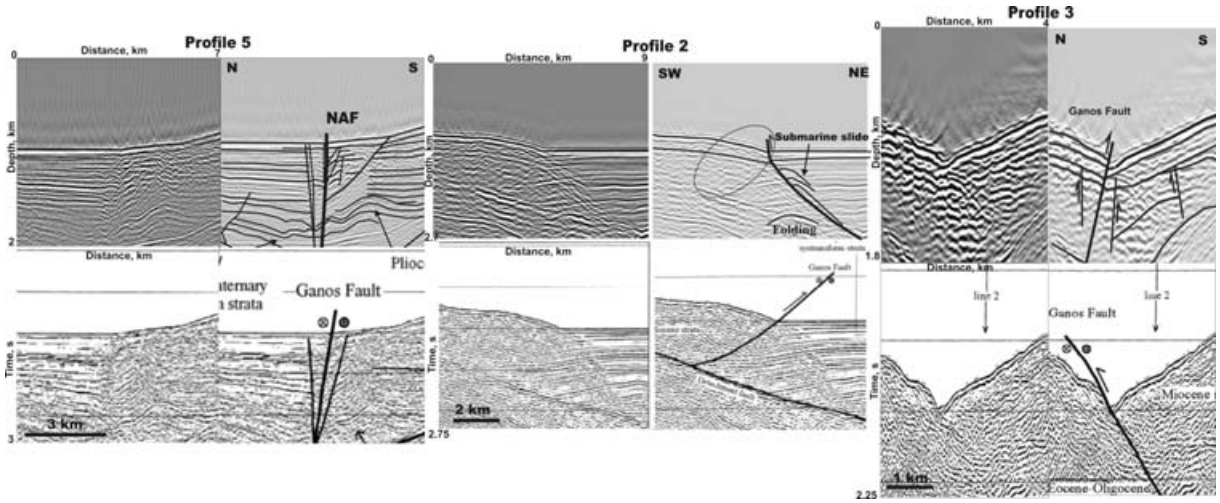


Figure 9. Illustration summarizes the main differences of the structural interpretation obtained from previous (Okay *et al.* 1999) and present studies.

© 2007 The Authors, *GJI*, **169,** 659–666
Journal compilation © 2007 RAS

Downloaded from https://academic.oup.com/gji/article-abstract/169/2/659/625546 by Suleyman Demirel Uni user on 17 April 2020

ACKNOWLEDGMENTS

We thank the MTA of Turkey and Dr Aral I. Okay (ITU, Turkey) for providing us the seismic data used in this study. We also thank to Dr Muhittin Gormus (SDU, Turkey) for his useful discussion. RG seismic reflection processing tools (Dr J. N. Louie, University of Nevada, Reno) was used to convert the seismic data to the images.

REFERENCES

Ambraseys, N.N., 2002. Seismic sea waves in the Marmara Sea region during the last 20 Centuries, *J. Seismol.*, **6**, 571–578.

Armijo, R., Meyer, B., Barka, A.A., Chabalier, J.B., Hubert-Ferrari, A. & Çakır, Z., 2000. The Fault breaks of the 1999 earthquakes in Turkey and the tectonic evolution of the Sea of Marmara: a summary, in 1999 İzmit and Düzce earthquakes: preliminary results, pp. 55–62, eds Barka, A.A., Kozacı, O., Akyüz, S.H., Altunel, E., İstanbul Technical University Publ., Istanbul.

Armijo, R., Meyer, B., Navarro, S., King, G. & Barka, A.A., 2002. Asymmetric slip partitioning In the Sea of Marmara pull-apart: a clue to propagation processes of the North Anatolian Fault? *Terra Nova*, **14**, 80–86.

Armijo, R. et al., 2005. Submarine fault scarps in the Sea of Marmara pull-apart (North Anatolian Fault): implications for seismic hazard in Istanbul, *G3*, **6**(3), 1–29.

Barka, A.A. & Kadınsky-Cade, K., 1988. Strike-slip fault geometry in Turkey and its influence on earthquake activity. *Tectonics*, **7**, 663–684.

Crampin, V. & Evans, R., 1986. Neotectonics of Marmara Sea region of Turkey, *J. Geol. Soc*, **143**, 343–348.

Demirbağ, E., Rangin, C., Xavier, L.P. & Şengör, C., 2003. Investigation of the tectonics of the Main Marmara Fault by means of deep-towed seismic data, *Tectonophysics*, **361**, 1–19.

Dix, C.H., 1965. Reflection seismic crustal studies: *Geophysics*, **30**, 1068–1084.

Ergün, M. & Özel, E., 1995. Structural relationships between the Sea of Marmara Basin and the North Anatolian Fault Zone, *Terra Nova*, **7**, 278–288.

Flerit, F., Armijo, R., King, G.C.P., Meyer, B. & Barka, A., 2003. Slip partitioning in the sea of Marmara pull-apart determined from GPS velocity vectors. *Geophys. J. Int.*, **154**, 1–7.

Görür, N. & Okay, A.I., 1996. Fore-arc origin of thr Thrace basin, northwest Turkey, *Geol. Rundsch.*, **85**, 662–668.

Honjas, W., 1995. Results of post pre-stack Migrations imaging the Hosgri fault, offshore Santa Maria Basin, CA., *MSc thesis*, Seismo lab., Univ. of Nevada, Reno, 109.

İmren, C., Le Pichon, X., Rangin, C., Demirbağ, E., Ecevitoğlu, B. & Görür, N., 2000. The North Anatolian Fault within the Sea of Marmara: a new interpretation based on multi-channel seismic and multy-beam bathymetry data, *Earth Planet. Sci. Lett.*, **186**, 143–158.

Jain, S. & Wren, A.E., 1980. Migration before stack–procedureand significance: *Geophysics*, **45**, 204–212.

Kanbur, Z., Louie, J.N., Chavez-Perez, Plank G. & Morey, D., 2000. Seismic Reflection Study of Upheaval Dome, National Park, Canyonlands, Utah, *J. Geophys. Res.-Planet.*, **105**(E4) 9489–9505.

Ketin, I., 1968. Relations between general tectonic features and the main earthquake regions in Turkey. *MTA Bull.*, **71**, 129–134.

Kopp, K.O., Pavoni, N. & Schındler, C., 1969. Geologie Thrakiens IV. Das Ergene Becken, *Beih. Geol. Jahrb.*, **76**, pp. 136.

Le Pichon, X., Taymaz, T. & Şengör, A.M.C., 1999. The Marmara Fault and the future İstanbul earthquake. in Karaca, M., Ural, D.N. (eds). *Proceedings of the International Conference on the Kocaeli earthquake, 17 August 1999*. Istanbul Technical University Press House, İstanbul. pp. 41–54.

Le Pichon, X., *et al.*, 2001. The active main Marmara fault, *Earth Planet Sci. Lett.*, **18**, 595–614.

Louie, J.N. & Qin, J., 1991. Subsurface imaging of the Garlock fault, Cantil Valley, California, *J. Geophys. Res.*, **96**, 14 461–14 479.

Louie, J.N., Clayton, R.W. & Le Bras, R.J., 1988. Three-dimensional imaging of steeply dipping structure near the San Andreas fault, Parkfield, California, *Geophysics*, **53**, 176–185.

McClusky, S.C. *et al.*, 2000. Global Positioning System constraints on plate kinematics and dynamics in the eastern Mediterranean and Caucasus, *J. Geophys. R.*, **105**, 5695–5719.

McKenzie, D.P., 1972. Active tectonics of the Mediterrenean region. *Geophys. J. Astron. Soc.*, **30**, 109–185.

Meade, B.J., Hager, B.H. & Reilinger, R.E., 2002. Estimates of seismic potential in the Marmara region from block models of secular deformation constrained by GPS measurements, *Bull.seism. Soc. Am.*, **92**, 208–215.

Okay, A.I., Demirbağ, E., Kurt, H., Okay, N. & Kucu, İ., 1999. An active, deep marine strike-slip basin along the North Anatolian fault in Turkey, *Tectonics.*, **18**(1), 129–147.

Okay, A.İ., Kalılar-Özcan, A., İmren, C., Boztepe-Güney, A., Demirbağ, E. & Kucu, İ., 2000. Active faults and evolving strike-slip basins in the Marmara Sea, northwest Turkey a multi-channel seismic reflection study. *Tectonophysics*, **321**, 189–218.

Okay, A.İ., Tüysüz, O. & Kaya, Ş., 2004. From transpression to transtension: changes in morphology and structure around a bend on the North Anatolian Fault in the Marmara region. *Tectonophysics*, **391**, 259–282.

Parke, J.R., Minshull, T.A., Anderson, G., White, R.S., McKenzie, D.P., Kuşcu, I., Görür, N. & Şengör, A.M.C., 1999. Active Faults in the Sea of Marmara, western Turkey, imaged by seismic reflection profiles, *Terra Nova*, **11**, 223–227.

Pınar, N., 1942. Geologie et meterologie sismuques du bassin de lamer de Marmara, *Univ. İstanbul Sci. Fac. Bull.*, **7**(3–4), 121–182.

Seeber, L., Emre, Ö., Cormier, M.-H., Sorlien, C.C., McHugh, C.M.G., Polonia, A., Özer, N. & Cağatay, N., 2004. Uplift and subsidence from oblique slip: the Ganos-Marmara bend of the North Anatolian Transform, Western Turkey, *Tectonophysics*, **391**, 239–258.

Smith, A.D., Taymaz, T., Oktay, F., Yüce, H., Alpar, B., Başaran, H., Jackson, J.A., Kara, S. & Şimşek, M., 1995. High-resolution seismic profiling in the Sea of Marmara (northwest Turkey): late Quetarnary sedimentation and sea-level changes, *Geol. Soc. Am. Bull.*, **107**, 923–936.

Sümengen, M. & Terlemez, İ., 1993. Stratigraphy of the Eocene sedimets from shoutwestern Thrace (in Turkish), *Maden Tetkik Arama Ens. Derg.*, **113**, 17–30.

Şengör, A.M.C., 1979. The North Anatolian transform fault: its age, offset and tectonic significance, *J. Geol. Soc. London.*, **136**, 269–282.

Şengör, A.M.C., Görür, N. & Şaroğlu, F., 1985. Strike-slip faulting and related basin formation in zones of tectonic escape: Turkey as a case study, in: *Strike-slip Deformation Basin Formation and Sedimentation*,Vol. 37, pp. 227–264, eds Biddle, K.T., Christie-Blick, N., *Soc. Econ. Paleontol. Mineral. Spec. Publ.*

Şengör, A.M.C., Demirbag, E., Tüysüz, O., Kurt, H., Görür, N. & Kuşcu, I., 1999. A preliminary note on structure of the Gulf of İzmit: implications for the westerly prolongation of the North Anatolian Fault, in Karaca, M., Ural, D.N.L., (eds), *Proceedings of the International Conference on the Kocaeli Earthquake*, 17 August, 1999, İstanbul University Press Houses, İstanbul. pp. 25–37.

Turgut, S., Türkaslan, M. & Perinçek, D., 1991. Evolution of the Thrace sedimentary basin and its hydrocarbon prospectivity, in *Generation accumulation and production of Europe's hydrocarbons*,Vol. 1, pp. 415–437, ed. Spencer, A.M., Spec. Publ. European Assoc. Petrol. Geoscientist.

Wong, H.K., Ludmann, T., Uluğ, A. & Görür, N., 1995. The Sea of Marmara: a plate boundary sea in an escape tectonic regime, *Tectonophysics*, **244**, 231–250.

Vidale, J.E., 1988, Finite-difference calculation of traveltimes, *Bull., Seis. Soc. Am.*, **78**, 2062–2076.

Yazman, M., 1997. Western Turkey poses exploration challenges on/offshore, *Leading Edge*, **16**(6), 897–899.

Yılmaz, Ö., 1987. Seismic data processing: investigations in Geophysics, Society of Exploration, Tulsa, **2**, 526.

Downloaded from https://academic.oup.com/gji/article-abstract/169/2/659/625546 by Suleyman Demirel Uni user on 17 April 2020